RSC Advances

Ecologically Green Conversion Coatings with Special Wetting Behaviors for Wax Prevention

Journal:	*RSC Advances*
Manuscript ID	RA-ART-01-2016-000611.R3
Article Type:	Paper
Date Submitted by the Author:	22-Feb-2016
Complete List of Authors:	Liang, Weitao; Beihang University, Zhu, Liqun; Beihang University, li, Weiping; Beihang University, Xu, Chang; Beihang University Liu, Huicong; Beihang University,
Subject area & keyword:	Films/membranes < Materials

Ecologically Green Conversion Coatings with Special Wetting Behaviors for Wax Prevention

*Weitao Liang, Liqun Zhu, Chang Xu, Weiping Li, Huicong Liu**

Key Laboratory of Aerospace Materials and Performance (Ministry of Education), School of Materials Science and Engineering, Beihang University, Beijing 100191, China

Corresponding Author

Huicong Liu

Key Laboratory of Aerospace Materials and Performance (Ministry of Education), School of Materials Science and Engineering, Beihang University, Beijing 100191, China

*E-mail address: liuhc@buaa.edu.cn

Tel: +86 1082317113. Fax: +86 1082317113.

Abstract

Superhydrophilicity and underwater superoleophobicity are fundamental issues in many applications for special wettable surfaces. In this work, the special wetting behaviors were achieved by an ecologically green wet chemical method. The prepared coatings with porous structure present superhydrophilicity and underwater superoleophobicity. The effects of the reaction conditions, such as pH values and conversion duration, on the morphology and wetting behaviors of the prepared coatings, were also studied. A wax deposition test based on cold-finger was carried out and good performance was investigated. A possible wax prevention mechanism is proposed, which can be calculated from water film theory. The corrosion resistance and stability of the prepared coatings were also measured. The prepared coatings with special wetting behaviors offer significant insight

for the design of anti-wax materials in water contained crude oil transition.

Key words: Ecologically green; Chemical conversion coating; Superoleophobicity; Wax prevention.

1 Introduction

Crude oil is the most important energy material in modern society, which known as the blood of industry. It is meaningful and exigent to guarantee adequate oil supplies.[1,2] Waxes are mainly paraffinic compounds that precipitated from crude oil at low temperature.[3] Wax deposited in the pipeline would reduce the effective cross area and raise the flow resistance, which leads to short supply and great economic losses.[4-6] Increase of pipeline pressure and decrease of pipeline temperature would further intensify wax deposition.[7, 8] It is essential to develop effective method to avoid wax deposition.

Many researchers have made great effort to avoid the wax deposition, such as microbial,[9] paraffin inhibitor,[10, 11] mechanical dewaxing[12] magnetic field dewaxing[13] and high-temperature dewaxing.[14] However, most of these methods are either inefficient or costly, and would cause environmental pollution. Therefore, great effort has been made to develop appropriate wax prevention methods, especially in costly and environmental friendly way.

Wax prevention coatings have attracted much attention due to the good performance, simple fabrication, low cost and wide application. Metal, glass, polymer and many other materials have been used to fabricate anti-wax coatings.[15-18] Some early researchers focused on the smooth coatings, such as glass and plastic.[15, 16] However, the wax prevention performance of those coatings was very poor. Some other researchers also developed coatings with special wetting behaviors for wax prevention, and good performance was investigated.[17, 18] In spite of the fact that its performance is relatively well, the preparation process would cause environmental pollution, and the wax prevention performance

was still low for application. For more and more people are aware of environmental issues, the environmental friendly method is urgently needed.[19] It is necessary and urgent to develop effective coatings for wax prevention, especially in facile, low-cost and environmental friendly way.

Our group has committed to develop efficient and low-cost wax prevention coatings for several years.[20-26] In the previous work, composite coating with fish-scale like morphology was prepared and excellent wax prevention performance was investigated.[22] In addition, an alternate current etching method was also employed to fabricate coatings with different surface morphology on carbon steels to prevent wax from deposition, and good performance was investigated.[23, 24] However, all the methods mentioned above would take power and make waste liquid. If the wax prevention efficiency is to be further improved, much more research needs to be done.

Phytic acid ($C_6H_{18}O_{24}P_6$) (PA), an inartificial and innoxious organic large molecular compound, consists of 24 oxygen atoms, 12 hydroxyl groups and 6 phosphate carboxyl groups.[27] The particular structure of PA has a powerful chelating capability with many metal ions, allowing it to form very stable complexes with multivalent cations.[28] PA is present in natural cereal grains and is employed as a vitamin component. The chelating process is non-toxic and low-cost, and necessitates no waste treatment to eliminate environmental pollution. Therefore, PA has been proposed as an environmental friendly reagent to prevent the surface of metal ions, such as Mg, Al, Zn, etc.[29-31] However, most of the previous work was focused on the corrosion resistance of the prepared conversion coating. As a common chemical conversion coating, the wetting behavior of the PA conversion coating has not been studied, and few people had employed it in wax prevention application.

In this work, a facile PA conversion method was employed to fabricate wax prevention coatings.

This conversion coating was achieved by simple wet chemical method without energy consumption and environmental pollution. The prepared conversion coatings with special porous structure show extreme superhydrophilicity and underwater superoleophobicity. The effect of the solution pH value and conversion duration, on the surface morphology and wetting behaviors of the conversion coatings, was also studied. Excellent wax prevention performance was investigated in a wax deposition test.[32] In addition, a possible wax prevention mechanism calculated from water film theory is proposed. Due to the obvious assets of facile fabrication, low cost and environmental friendly, the prepared PA conversion coating is expected to wide application in petroleum industry.

2 Experimental sections

2.1 Materials

The $ZnSO_4 \cdot 7H_2O$, $Al_2(SO_4)_3 \cdot 18H_2O$ and $KAl(SO_4)_2 \cdot 12H_2O$ were purchased from Xilong (AR, China) and used as received. The surfactant, PA and tri-ethanolamine (TEA) were purchased from Beijing Chemical works (AR, China). A3 carbon steels with the size of 20 mm×40 mm×2 mm were used as substrates. The A3 carbon steels were ultrasonically cleaned in acetone and then rinsed with deionized water sequentially before use. The crude oil for wax deposition test was from Daqing Oilfield (in Heilongjiang province, China). The main characteristics of the waxy crude oil are shown in Table 1, indicating a typical waxy crude oil. The crude oil contains about 50 wt% water, which is consistent with most of the actual situations.

2.2 Preparation of the chemical conversion coating

The Zn coating was prepared by electroplate method in the bath containing 2 M $ZnSO_4 \cdot 7H_2O$, 0.05 M $Al_2(SO_4)_3 \cdot 18H_2O$, 0.1 M $KAl(SO_4)_2 \cdot 12H_2O$ and 0.02 M surfactant. The solvent of the

electroplate bath is deionized water. The conversion coating was prepared on Zn coated A3 carbon steel in the conversion solutions with different pH values by immersing 20 min at 40 ^{o}C. The pH value of conversion solution can be controlled by adjusting the TEA dose. After immersion, the specimens were thoroughly washed using running deionized water, dried at room temperature and then measured.

2.3 Wax deposition test

The wax deposition procedure was simulated in the laboratory using a self-designed apparatus based on the cold-finger method.[32] In the wax deposition test, crude oil was heated to 80 ℃ in a water bath and stirred thoroughly (ω=20 rad·s^{-1}) to ensure complete dissolution and well-distribution of wax. Then the specimens were fixed onto the inner wall of the container. After the oil was kept at 80 ℃ for 0.5 h, it was cooled by circulating water cooling (water temperature is 25 ℃). It takes about 2 hours until the oil temperature decreased to 25 ℃.

The quantitative determination of the wax prevention deposition weight, DW in abbreviation, was calculated according to Eq. (1):[22]

$$DW = \frac{(W_t - W_0)}{S_0} \times 100\% \quad (1)$$

where W_t is the weight of the wax deposited specimen; W_0 is the weight of the original specimen; S_0 is the surface area of specimen. For anti-wax treatment specimens, a less DW value means a better wax prevention property.

2.4 Characterizations

A scanning electron microscope (SEM, JSM-7500F, JEOL Ltd., Japan) was used to observe the surface morphology of the obtained specimens. Before the observation, the specimens were sputter-coated with Pt under the vacuum conditions for electric conduction. Fourier transform

infrared (FTIR) spectra was collected on a FTIR spectrometer (NEXUS-470, Nicolet Co.) using the KBr method and transmission mode. Digital images of the specimens before and after the wax deposition test were obtained by a digital camera (Olympus, E-PL1). The contact angles of bare water on the specimens were measured using a contact angle meter (DSA 20, Krüss Instruments GmbH) on five different positions for each surface. The volume of an individual droplet in all measurements was 5 μL. The contact angles of oil on the specimens in water were also measured using the contact angle meter (DSA 20, Krüss Instruments GmbH) via underwater oil contact angles (OCA) test.[22, 23] The specimens were upside down in a water-filled glass container because the density of oil was lower than water. First, specimens were immersed in hot water (T ≈ 80 ^{o}C to keep crude oil at the liquid state), and then a crude oil droplet was gently injected by a micro syringe on the surfaces. The OCA can be calculated by Eq. (2):[33]

$$\tan\frac{\theta}{2}=\frac{2h}{D} \quad (2)$$

where θ is the OCA, h is the height of the oil droplet and D is the length of the oil droplet contact the specimen surface, which can all be measured directly in the digital image of the OCA.

The effects of the prepared conversion coatings on the corrosion protection properties of the samples were evaluated by electrochemical impedance spectroscopy (EIS) and salt spray test. The EIS analysis was carried out in a conventional three-electrode cell including saturated Ag/AgCl as reference electrode, Platinum as counter electrode and the prepared sample as working electrode. Measurements were performed on 1 cm^2 of the prepared sample immersed in the 3.5 wt.% NaCl

solutions. The salt spray tests were conducted in SF850 salt spray cabinet (Atlas Electric Devices). The pH and NaCl concentration of salt fog were 7 and 5 wt.%, respectively.

The stability of the prepared surface was investigated by a flush test. The prepared sample was flushed by deionized water from 50 cm upon the surface at a speed of 5 mL per second. After a continuous test of several hours, the sample was moved away to test the CAs at the place where the water flush on it to evaluate the flush resistance.

3 RESULTS AND DISCUSSION

3.1 Structure characterization, wetting behaviors and chemical characterization.

The pH value of conversion solution plays a key role in the formation of conversion coatings.[31] How the pH value influences the conversion coatings, especially on the morphology and wetting behaviors, was studied and the results were shown in Figure 2 and Figure 3.

Figure 2 shows the SEM images of the PA conversion coatings attained under different solution pH value. Insets are the high resolution SEM images of the corresponding coatings. It can be seen that, for the solution with series pH value of 2.0, 3.0, 4.0 and 5.0, the specimens present different surface morphology (Figure 2 (A-D)). There is no obvious conversion coating formed in the solutions with pH of 2.0, as shown in Figure 2 (A). It can be ascribed to the excess high concentration H^+, which leads to a passive film on the Zn coating and stops the subsequent reactions. For the solution with pH of 3.0, the specimen is entirely covered, but the microstructure of the coating surface is fragmentized and uneven, as shown in Figure 2 (B). For the solution pH is increased to 4.0, the microstructure of the coating surface becomes integrated and uniform (Figure 2 (C)). As pH increasing to 5.0, the concentration of H^+ decreases and causes reactions to slow down.

There is almost no conversion coating on the specimen surface, as shown in Figure 2 (D). (The SEM images of the prepared surface attained with pH value of 1.0 and 6.0 can be seen in Supporting Information Figure S1)

The contact angles (CAs) and underwater oil contact angles (OCAs) are closely related to the surface morphology.[34] The conversion coatings attained under different pH value present different CAs and OCAs for different morphology. The digital images of CAs and OCAs are measured and shown in Figure 3. The CA decreases from 81.2±1.2^{o} to 34.5±1.1^{o} with the solution pH value increasing, as shown in Figure 3 (A) (a-b). At the same time, the underwater OCA increases from 133.0±2.0^{o} to 151.9±1.6^{o}, as shown in Figure 3 (B) (a-b). With the solution pH value increasing to 4.0, the conversion coating presents superhydrophilicity with CA of about 0^{o}, and the underwater OCA further increases to 163.2±1.4^{o}, which can be considered to superoleophobicity. The special wetting behavior of superhydrophilicity and underwater superoleophobicity are attributed to the porous structure of the conversion coating.[35] As the solution pH value further increases, the concentration of H^{+} in the conversion solution decreases and the porous structure disappear. The conversion coatings return to hydrophobic again as shown in Figure 3 (A) (d). It can be concluded that when the solution pH value is 4.0, the conversion coatings would present superhydrophilicity and underwater superoleophobicity for the porous structure.

The conversion coating attained at pH value of 4.0 shows superhydrophilicity and underwater superoleophobicity, which greatly arouse our interest. To further investigate the composition of the prepared coating, the EDS pattern and FTIR spectrum are measured and the results are shown in Figure 4. Figure 4 (A) shows the EDS pattern of the conversion coating, indicating that O, P and Zn are detected. The broad vibration bands at 1126 cm^{-1}, 1290 cm^{-1} and 1369cm^{-1} in the FTIR spectrum

(Figure 4 (B)) would be characteristic of P=O. Vibration bands at 996 cm^{-1} and 835 cm^{-1} are associated with the P-OH and C-P-O stretching bands in PA, respectively. While the intensive vibration bands among 2800 cm^{-1} and 3800 cm^{-1} are associated to OH in PA. From the results of EDS pattern and FTIR spectrum, it may be estimated that after immersing in PA, a layer of PA conversion coating was fabricated on the specimen.

As a matter of fact, PA is consisted of 24 oxygen atoms, 12 hydroxyl groups and 6 phosphate carboxyl groups.[27, 28] The ionization equations of PA in the water were as follows:[29]

$$RH_{12} + H_2O \leftrightarrow RH_{11}^{-} + H_3O^{+}$$

$$RH_{11}^{-} + H_2O \leftrightarrow RH_{10}^{2-} + H_3O^{+}$$

($R=C_6H_6O(PO_3)_6$)

According to the results of EDS and FTIR analyze, the formation for the conversion coatings can be speculated as shown in Figure 4 (C).

On the authority of previous literatures[27, 28] and above reactions, the formation process of the conversion coating can be calculated as follows. At first, the specimen was immersed in the conversion solution, dissolution of the Zn occurred, forming Zn^{2+}, accompanied by the intense formation of H_2. The anodic reaction was the dissolution of Zn and the cathode reaction was the reduction of H^{+}. Then the Zn^{2+} reacted with the phytate groups to form insoluble compounds, which is called chelate process. The concentration of insoluble compounds increased as the reaction happened. Finally, the concentration of insoluble compounds increased to a certain value and gradually deposited on the substrate surface to form the conversion coating.

3.2 The growing process of the conversion coatings.

To further investigate the growing process of the prepared chemical conversion coatings, the

following experiments were carried out. Figure 5 shows the surface morphology of the prepared conversion coatings with different treatment durations. The pH value of the conversion solution is 4.0.

Before immersing in the conversion solution, many hexagon grains can be seen in Figure 5 (A), which are corresponded to the typical shape of Zn.[36] (Detailed SEM images and high-resolution SEM images of the PA conversion coatings with different conversion time can be seen in Supporting Information Figure S2) The surface of the Zn grain is flat. After immersing in the PA conversion solution for 1 min, the Zn grains can still keep their hexagon shape, as shown in Figure 5 (B). We can also find that there are some small particles growing on the surface of the Zn grains, which can be speculated to the first generated products. The surfaces also become a little rough, as shown in Figure 5 (B). As the conversion time increased to 5 min, more products appeared on the surface of the Zn grains, as shown in Figure 5 (C). The Zn grains are completely covered by the new generated products after immersing in conversion solution for 10 min. The new generated particles combined with each other and formed porous structure on the surface of the specimen, as shown in Figure 5 (D). The corresponding EDS pattern of the new particles shown in Supporting Information Figure S3 indicates that the new particles are also RHn-Zn ($R=C_6H_6O(PO_3)_6$. The porous structure is the key to achieve surperhydrophilicity for it can make hydrophilic surface more hydrophilic.[35] The formation of the porous structure can be attributed to the H_2 which would form because of the reaction between the Zn and PA during the conversion process.[37] The huge amount H_2 transiting the surface layers resulted in the formation of porous structure. Figure 5 (E) shows that after immersing in conversion solution for 20 min, the new generated particles uniformly distribute on the surface with porous structure. The new generated particles grow larger with the immersing time increasing, and the

specimen surface became more porous, as shown in Figure 5 (F) and (G). In conclusion, 20 min is appropriate time to get both superhydrophilic and stable conversion coating.

It can be concluded that when the pH value of conversion solution was 4.0, the prepared conversion coating formed a special porous structure, which can be detected to R-Zn ($R=C_6H_6O(PO_3)_6$). This porous structure and high surface energy composition give the prepared conversion coating special wetting behavior: superhydrophilicity and underwater superoleophobicity, which have been proved to be conductive to wax prevention in petroleum industry.[38]

3.3 Wax prevention performance.

To investigate the wax prevention performance, a wax deposition test was carried out and the results were shown in Figure 6. Three Zn coated carbon steels and three prepared conversion coatings were employed to investigate the wax prevention performance. Figure 6 (A) shows the schematic diagram of the cold-finger wax deposition test, indicating that the deposition apparatus include four basic parts: temperature controller system (thermostat water bath and circulating water-cooling), stirring system, water-contained waxy crude oil and washing system. The Figure 6 (C) shows the full view of three Zn coatings after wax deposition test, and Figure 6 (D) shows the full view of three conversion coatings. Obviously, the Zn coatings were covered with thick layer of wax oil mixtures while the conversion coatings were undefiled with a little wax on the surfaces. The wax deposition weights (DWs) of different coatings were also calculated and the results were shown in Figure 6 (B), indicating that Zn coating and the prepared conversion coating have great difference in wax prevention performance. The DW value for Zn coating is 5.432±0.204 g/dm^2, indicating really terrible wax prevention property, while the DW value of 0.096±0.012 g/dm^2 for the prepared conversion coating showing good wax prevention property. By the way, the digital images of the

bare A3 carbon steels after wax deposition test in Supporting Information Figure S4 indicate that bare A3 carbon steels present very bad performance in wax deposition test.

To better understand the mechanism of the excellent wax prevention ability, the specific wetting behavior of the prepared conversion coating in air and underwater were systematic studied. Figure 7 (A) shows the rapidly wetting process of water droplet on the prepared conversion coating, which indicates that the conversion coating is superhydrophilic in the air. A superhydrophilic surface usually presents superoleophobicity underwater, [22, 38] and the results of underwater OCA in Figure 7 (B) further confirm this view. The underwater OCA was about 162.6°. The underwater oil rolling angle of 2.8° indicates that only a tiny deflection can make the oil drop roll away.

It is known that crystallization of wax is a kinetic process, the onset of which can be described by classical homogeneous nucleation theory.[39] In the water-contained crude oil system, the crystallization of wax can be divided into two stages: nucleation and crystal growth. The nucleation speed (v_1) and the crystal growth speed (v_2) can be calculated according to Eq. (4) and (5), respectively[40]:

$$v_1 = k\frac{(c - c_e)}{c_e} \quad (4)$$

$$v_2 = \frac{D}{\delta}A(c - c_e) \quad (5)$$

where c is the concentration of supersaturated solution, c_e is the concentration of the saturated solution, k is a constant, D is the solute diffusion coefficient, δ is the diffusion distant and A is the surface area of the nucleation. In oil pipeline, temperature near the pipeline inwall is much lower than the pipeline center, which resulted in a lower c_e, and further leaded to higher v_1 and v_2.[7, 8, 39] That is why the pipeline inwall is easier to form wax nucleus. While in this work, for

superhydrophilicity, the water would rapidly cover the whole conversion coating surface and form a continuous water film, as shown in Figure 7 (A), which can stop the wax nucleus forming on the surface or bonding in the surface. The water film acted as a barrier to prevent the oil and the PA conversion coating contact. For the small bonding force between the water film and the oil, the new generated wax nucleus would easily roll away with the flowing crude oil fast. On this basis, the rapid wetting process of water and fast rolling of oil are the two key points for the wax prevention. The results in this work coincide with those obtained previous.[22, 23]

3.4 Corrosion resistance and stability tests.

It is known that good corrosion resistance and stability are always required for the hot, damp and salty environment during the transition, which causes reinforcement rusting and thermal damage.[40] Thus the corrosion resistance and stability of the prepared PA conversion coating were also investigated in this work.

To investigate the anti-corrosion property of the prepared conversion coatings, we characterized bare A3 carbon steel, Zn coating and prepared conversion coating with potentiodynamic polarization in 3.5 wt.% NaCl solution. The potentiodynamic polarization curves of electrical parameters of the corrosion potentials (E_{corr}), corrosion current densities (i_{corr}) and polarization resistance (R_p) are presented in Figure 8 (A) and Table 2, respectively. The result of Figure 8 (A) indicates that comparing to the bare carbon steel and Zn coating, an obvious corrosion current densities decrease can be observed in conversion coating, indicating the increase of corrosion consistent. It can be attributed to the conversion coating that provide a passive treatment and reduce the formation of corrosion products. Furthermore, the results of Table 2 indicated that with the conversion coating, the corrosion current density (i_{corr}) is lower than the Zn coating and bare A3 carbon steel while the

polarization resistance (R_p) is greater, indicating that the conversion coating is able to offer higher corrosion protection. In conclusion, the increasing of corrosion resistance can be contributed that the conversion coating formed a barrier layer, which can effectively prevent air and solution infiltration and increase the anti-corrosion stability.

The salt spray enlarged rusty test was used to estimate the anti-corrosion performance of Zn coatings and prepared conversion coatings. The results after 24 h of salt spray tests were shown in Figure 8 (B). The bare A3 carbon steel (Figure 8 (a)) is absolutely covered by the red corrosion products and the Zn coating (Figure 8(b)) also has heavy corrosion with white corrosion products on the whole surface, while the prepared conversion coating (Figure 8(c)) is almost clean with a little white corrosion products on the sample edge. It is seen that the prepared conversion coating possesses comparative anticorrosion resistance to that of Zn coating. The corrosion of the enlarged rusty of bare A3 carbon steel is rather terrible. Therefore, the prepared conversion coating has a beneficial effect on the anticorrosion property of the samples.

To further investigate the stability, a flush test was also carried out and the result was shown in Figure 8 (D). The result shows that after a continuous flush test of 48 hours, the prepared sample can also keep superhydrophilic, which indicates a good flush resistance. The results of the flush test indicate that the prepared conversion coating has a good performance in flush resistance. A pipe-like model was also developed to test the stability of prepared coating, as shown in Supporting Information Figure S5 (A), and the result in Figure S4 (B) indicates good performance. Because of the condition limitation, it is hard for us to test the prepared coating in real crude oil pipeline, but the results in this work can confirm the practicability to some extent.

Above all, it can be concluded that the prepared conversion coating present extreme stability

which is very meaningful in industry application.

4 Conclusions

In this work, a facile wet chemical method was employed to prepare wax prevention coatings. Zn coated A3 carbon steel was immersed in a PA conversion solution for 20 min at 40 ^{o}C. The prepared coatings present special wetting behavior of superhydrophilicity and underwater superoleophobicity. The effects of the reaction conditions, such as conversion time and pH values, on the morphology and wetting behavior of the prepared coatings, were also studied. The prepared coatings present good performance in cold-finger wax deposition test. A possible wax prevention mechanism calculated from water film theory is proposed. Besides, this PA conversion method without any energy consumption and polluted liquid is good to environment protection. This environmental friendly method offers significant insight for the design of antiwax materials in water-contained crude oil transition.

Author information

Corresponding Author

*E-mail: liuhc@buaa.edu.cn. Tel: +86 1082317113. Fax: +861082317113.

Author Contributions

All authors contributed to the development of the experimental design, the discussion of the results, and the preparation of the manuscript. All authors have given approval to the final version of the manuscript.

Notes

The authors declare no competing financial interest.

Acknowledgments

The authors are very grateful to the support from the National Natural Science Foundation of China (Grant No. 51401011).

References

(1) Venkatesan, R.; Ostlund, J. A.; Chawla, H.; Wattana, P.; Nyden, M.;Foler, H. S. The effect of asphaltenes on the gelation of waxy oils. *Energy Fuels.* **2003**, 17 (6), 1630–1640.

(2) Martínez-Palou, R.; de Lourdes Mosqueira, M.; Zapata-Rendón, B.; Mar-Juárez, E.; Bernal-Huicochea, C.; de la Cruz Clavel-López, J.; Aburto, J. Transportation of heavy and extra-heavy crude oil by pipeline: A review. *J. Pet. Sci. Eng.* **2011**, 75(3), 274-282.

(3) Burger, E. D.; Perkins, T. K.; Striegler, J. H. Studies of wax deposition in the trans Alaska pipeline. *J. Petroleum Technol.* **1981**, 33, 1075–1087.

(4) Weingarten, J. S.; Euchner, J. A. Methods for predicting wax precipitation and deposition. *SPE Prod. Eng.* **1988**, 3(01), 121-126.

(5) Azevedo, L. F. A.; Teixeira, A. M. A critical review of the modeling of wax deposition mechanisms. *Pet. Sci. Technol.* **2003**, 21(3-4), 393-408.

(6) Jennings, D. W.; Weispfennig, K. Effects of shear and temperature on wax deposition: Cold finger investigation with a Gulf of Mexico crude oil. *Energy & Fuels*. 2005, 19(4), 1376-1386.

(7) Elsharkawy, A. M.; Al-Sahhaf, T. A.; Fahim, M. A. Wax deposition from Middle East crudes. *Fuel*. **2000,** *79*(9), 1047-1055.

(8) Zhao, Y.; Kumar, L.; Paso, K.; Safieva, J.; Sariman, M. Z. B.; Sjöblom, J. Gelation behavior of model wax–oil and crude oil systems and yield stress model development. *Energy Fuels.* **2012**, 26(10), 6323-6331.

(9) He, Z.; Mei, B.; Wang, W.; Sheng, J.; Zhu, S.; Wang, L.; Yen, T.F. A Pilot Test Using Microbial

Paraffin-Removal Technology in Liaohe Oilfield. *Pet. Sci. Technol.* **2003**, 21, 201-210.

(10) Taraneh, J. B.; Rahmatollah, G.; Hassan, A. Effect of wax inhibitors on pour point and rheological properties of Iranian waxy crude oil. *Fuel Process. Technol.* 2008, 89(10), 973-977.

(11) Bello, O. O.; Fasesan, S. O.; Teodoriu, C. An evaluation of the performance of selected wax inhibitors on paraffin deposition of Nigerian crude oils. *Pet. Sci. Technol.* 2006, 24(2), 195-206.

(12) Jorda, R. M. Paraffin deposition and prevention in oil wells. *J. Petroleum Technol.* **1966**, *18*(12), 1-605.

(13) Goncalves, J.L.; Bombard, A. J. F.; Soares, D. A. W.; Alcantara, G. B. Reduction of Paraffin Precipitation and Viscosity of Brazilian Crude Oil Exposed to Magnetic Fields. *Energy Fuels.* **2010**, 24, 3144–3149.

(14) Li, H.; Zhang, J.; Song, C. The influence of the heating temperature on the yield stress and pour point of waxy crude oils. *J. Pet. Sci. Eng.* **2015**, 135, 476-483.

(15) Li, M.; Su, J.; Wu, Z.; Yang, Y.; Ji, S. Study of the mechanisms of wax prevention in a pipeline with glass inner layer. *Colloids Surf. A.* **1997**, 123, 635-649.

(16) Chen, B.; Ju, G.; Sakaia, E.; Qiu, J. Underwater low adhesive hydrogel-coated functionally integrated device by a one-step solution-immersion method for oil–water separation. *RSC Adv.* **2015**, 5, 87055-87060.

(17) Paso, K.; Kompalla, T.; Askeb, N.; Rnningsen, H. P.; Øye, G.; Sjöbloma, J. Novel Surfaces with Applicability for Preventing Wax Deposition-A review. *J. Dispersion Sci. Technol.* **2009**, 30, 757-781.

(18) Quintella, C. M.; Musse, A.P.S.; Castro, M.T.P.O.; Scaiano, J.C.; Mikelsons, L.; Watanabe, Y.N. Polymeric Surfaces for Heavy Oil Pipelines To Inhibit Wax Deposition- PP, EVA28, and HDPE.

Energy Fuels, **2006**, 20 (2), 620–624.

(19) De Klerk, A. Environmentally friendly refining: Fischer–Tropsch versus crude oil. *Green Chem*. **2007**, *9*(6), 560-565.

(20) Guo, Y.; Li, W.; Zhu, L.; Liu, H. An excellent non-wax-stick coating prepared by chemical conversion treatment. *Mater. Lett.* **2012**, 72, 125-127.

(21) Guo, Y.; Li, W.; Zhu, L.; Wang, Z.; Liu, H. Phosphoric chemical conversion coating with excellent wax-repellent performance. *Appl. Surf. Sci.* **2012**, 259, 356-361.

(22) Liang, W.; Zhu, L.; Li, W.; Yang, X.; Xu, C.; Liu, H. Bioinspired Composite Coating with Extreme Underwater Superoleophobicity and Good Stability for Wax Prevention in the Petroleum Industry. *Langmuir.* **2015**, 31(40), 11058-11066.

(23) Wang, Z.; Zhu, L.; Liu, H.; Li, W. Bioinspired in Situ Growth of Conversion Films with Underwater Superoleophobicity and Excellent Self-Cleaning Performance. *ACS Appl. Mater. Interfaces.* **2013**, 5 (21), 10904–10911

(24) Liang, W.; Zhu, L.; Li, W.; Liu, H. Facile fabrication of flower-like CuO/$Cu(OH)_2$ nanorods film with tunable wetting transition and excellent stability. *RSC Adv.* **2015**, 5, 38100 – 38110

(25) Wang, Z.; Zhu, L.; Liu, H.; Li, W. Investigation on the paraffin prevention performance of lanthanum-modified zinc powder. *Appl. Surf. Sci.* **2012**, 259, 1-6.

(26) Wang, Z.; Zhu, L.; Liu, H.; Li, W. A conversion coating on carbon steel with good anti-wax performance in crude oil. *J. Pet. Sci. Eng.* **2013**, 112, 266-272.

(27) Liu, J. R.; Guo, Y. N.; Huang, W. D. Study on the corrosion resistance of phytic acid conversion coating for magnesium alloys. *Surf. Coat. Technol.* **2006**, *201*(3), 1536-1541.

(28) Gao, L.; Zhang, C.; Zhang, M.; Huang, X.; Jiang, X. Phytic acid conversion coating on Mg–Li

alloy. *J. Alloys Compd.* **2009**, *485*(1), 789-793.

(29) Liang, C. H.; Zheng, R. F.; Huang, N. B.; Xu, L. S. Conversion coating treatment for AZ31 magnesium alloys by a phytic acid bath. *J. Appl. Electrochem*. **2009**, 39(10), 1857-1862.

(30) Zhang, R. F.; Xiong, G. Y.; Hu, C. Y. Comparison of coating properties obtained by MAO on magnesium alloys in silicate and phytic acid electrolytes. *Curr. Appl Phys.* **2010**, 10(1), 255-259.

(31) Martin, C. J.; Evans, W. J. Phytic acid-metal ion interactions. II. The effect of pH on Ca (II) binding. *J. Inorg. Biochem.* **1986**, *27*(1), 17-30.

(32) Kasumu, A. S.; Mehrotra, A. K. Solids Deposition from Wax–Solvent–Water "Waxy" Mixtures Using a Cold Finger Apparatus. *Energy Fuels*. **2015,** 29(2), 501-511.

(33) Li, J.; Cheng, H.; Chan, C.; Ng, P, F.; Chen, L.; Fei, B.; John, H. X. Superhydrophilic and underwater superoleophobic mesh coating for efficient oil–water separation. *RSC Adv.* **2015**, 5, 51537-51541.

(34) Zhang, M.; Zang, D.; Shi, J.; Gao, Z.; Wang, C.; Li, J. Superhydrophobic cotton textile with robust composite film and flame retardancy. *RSC Adv*. **2015**, 5, 67780-67786.

(35) Wenzel, R. N. Surface roughness and contact angle. *J. Phys.Chem.* **1949**, 53, 1466–1467.

(36) Nakano, H.; Oue, S.; Miki, T.; Kobayashi, S.; Fukushima, H. Effect of polyethylene glycol on the morphology of Zn electrodeposited on steel sheet. *ISIJ international*. **2006**, 46(1), 106-110.

(37) Zhang, R. F.; Zhang, S. F.; Duo, S. W. Influence of phytic acid concentration on coating properties obtained by MAO treatment on magnesium alloys. *App. Sur. Sci*. **2009**, *255*(18), 7893-7897.

(38) Wang, Z.; Jiang, X.; Cheng, X.; Lau, C.H.; Shao, L. Mussel-Inspired Hybrid Coatings that Transform Membrane Hydrophobicity into High Hydrophilicity and Underwater Superoleophobicity

for Oil-in-Water Emulsion Separation. *ACS Appl. Mater. Interfaces.* **2015**, 7, 9534–9545.

(39) Zougari, M. I.; Sopkow, T. Introduction to crude oil wax crystallization kinetics: process modeling. *Ind. Eng. Chem. Res.* **2007**, 46(4), 1360-1368.

(40) Swartwout, R. T.; Ho, T. Chacterzation of carbonate precipitation and scale formation in solids-free clear brines. *Society of Petroleum Engineers*. **1992**, 23811.

(41) Efird, K. D.; Jasinski, R. J. Effect of the crude oil on corrosion of steel in crude oil/brine production. *Corrosion*. **1989**, 45(2), 165-171.

(42) El-Sayed, A. R.; Mohran, H. S.; El-Lateef, H. M. A. Corrosion study of zinc, nickel, and zinc-nickel alloys in alkaline solutions by Tafel plot and impedance techniques. *Metall. Mater. Trans. A.* **2012**, 43(2), 619-632.

Table 1 Characteristics of the waxy crude oil.

parameter	value
Wax (wt%)	≈26
Resins (wt%)	≈12
Water (wt%)	≈50
Pour point (^{o}C)	≈32

Table 2 The parameters derived from the potentiodynamic polarization curves in 3.5 wt.% NaCl solution.

Specimen	E_{corr}(V/SCE)	I_{corr}(A/cm^2)	R_p(Ω/cm^2)
Conversion coating	-0.9638±0.03	$7.94\pm0.10\times10^{-8}$	$1.21\pm0.40\times10^{7}$
Zn coated carbon steel	-0.7785±0.03	$3.87\pm0.25\times10^{-7}$	$2.01\pm0.31\times10^{6}$
A3 carbon stell	-0.5951±0.03	$9.23\pm0.14\times10^{-7}$	$6.44\pm0.35\times10^{5}$

Figure 1. (A) SEM image of the Zn coating, (insets are the digital images of the CA and underwater OCA); (B) SEM image of the conversion coating, (insets are the digital images of the CA and underwater OCA); (C) the schematic diagram of the Zn coating in wax deposition test; (D) the schematic diagram of the conversion coating in wax deposition test.

Figure 2. The SEM images of conversion coatings attained under different solution pH value: (A) 2.0; (B) 3.0; (C) 4.0; (D) 5.0. Insets are the high resolution SEM images of the corresponding coatings.

Figure 3. (A) The CA digital images of the PA conversion coatings attained under different solution pH value: (a) 2.0; (b) 3.0; (c) 4.0; (d) 5.0. (B) The underwater OCA digital images of the conversion coatings attained under different solution pH value: (a) 2.0; (b) 3.0; (c) 4.0; (d) 5.0.

Figure 4. The (A) EDS pattern and (B) FTIR spectrum of the prepared conversion coating at solution pH value of 4.0; (C) Schematic illustration for the chelate process of PA on the Zn coating.

3.2 The coating formation process.

Figure 5. The SEM images of PA conversion coatings with different conversion time: (A) 0 min; (B) 1 min; (C) 5 min; (D) 10 min; (E) 20 min; (F) 30 min; (G) 60 min.

Figure 6. (A) Schematic diagram of cold-finger wax deposition test; (B) The average wax deposition weight of different coatings; (C) the digital images of Zn coatings after wax deposition test; (D) the digital images of the prepared conversion coatings after wax deposition test.

Figure 7. Digital images of: (A) Rapid wetting process and (B) Fast rolling process; (C) the wax prevention mechanism diagram of the prepared conversion coating.

Figure 8. (A) Potentiodynamic polarization curves of (a) prepared conversion coating, (b) Zn coated carbon steel and (c) bare A3 carbon steel. (B) The salt spray test results of different specimens: (a)

A3 carbon steel; (b) Zn coated sample and (c) prepared conversion coating. (C) The schematic diagram of flushing test. (D) The contact angles of prepared samples after flushing for different dyration.

Graphical abstract

(A) SEM image of the Zn coating, (insets are the digital images of the CA and underwater OCA); (B) SEM image of the conversion coating, (insets are the digital images of the CA and underwater OCA); (C) the schematic diagram of the Zn coating in wax deposition test; (D) the schematic diagram of the conversion coating in wax deposition test.

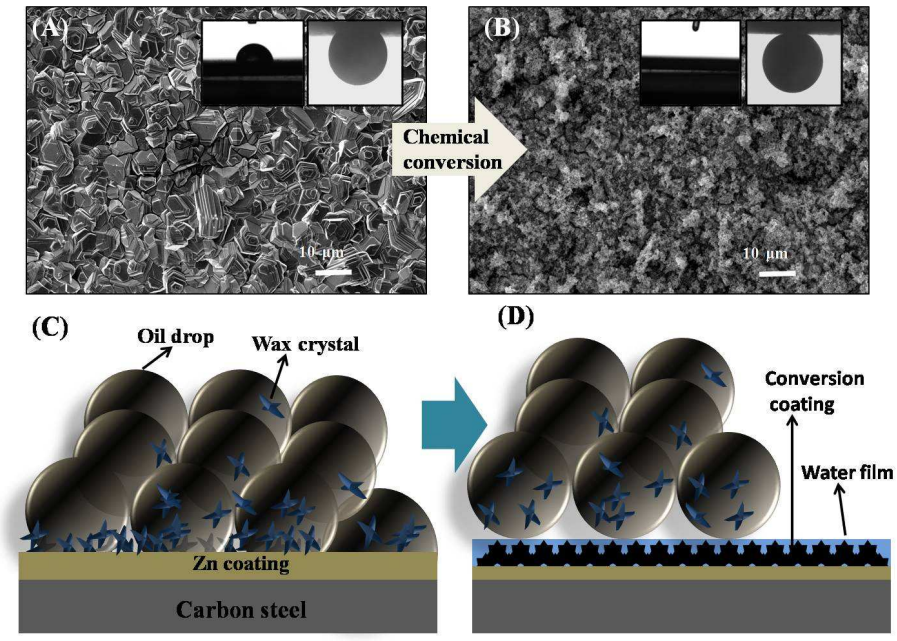

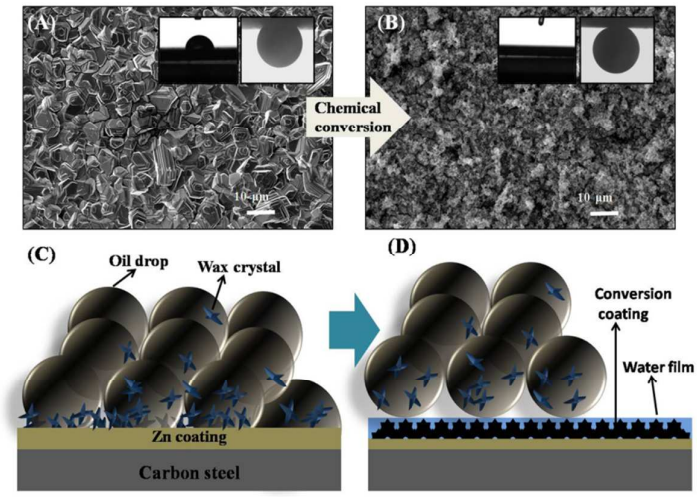
(A)
(B)
Chemical conversion
10 μm
10 μm
(C)
Oil drop
Wax crystal
(D)
Conversion coating
Water film
Zn coating
Carbon steel

Figure 1

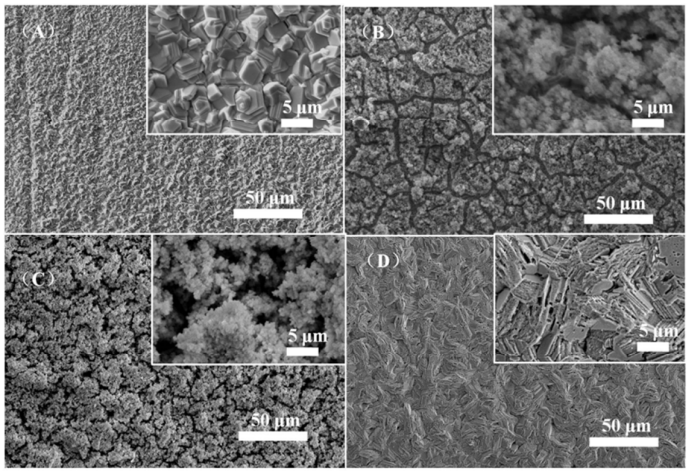

Figure 2

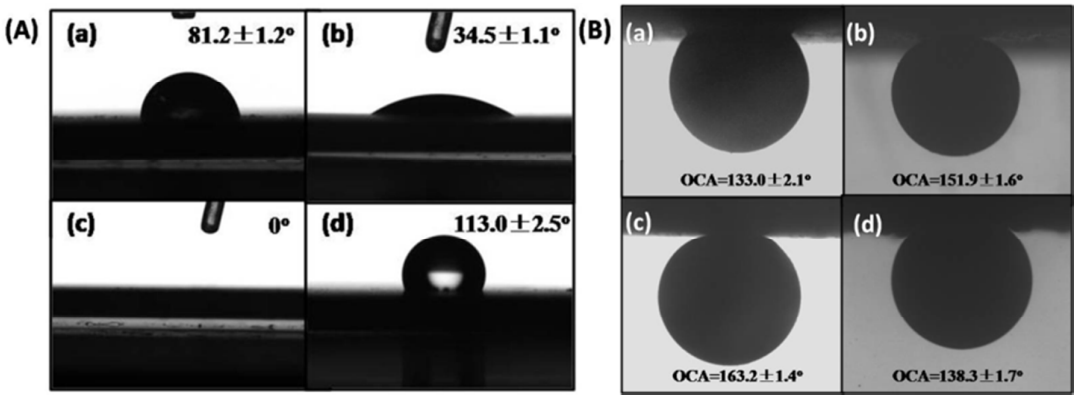
(A)
(a)
81.2±1.2°
(b)
34.5±1.1°
(c)
0°
(d)
113.0±2.5°
(B)
(a)
OCA=133.0±2.1°
(b)
OCA=151.9±1.6°
(c)
OCA=163.2±1.4°
(d)
OCA=138.3±1.7°

Figure 3

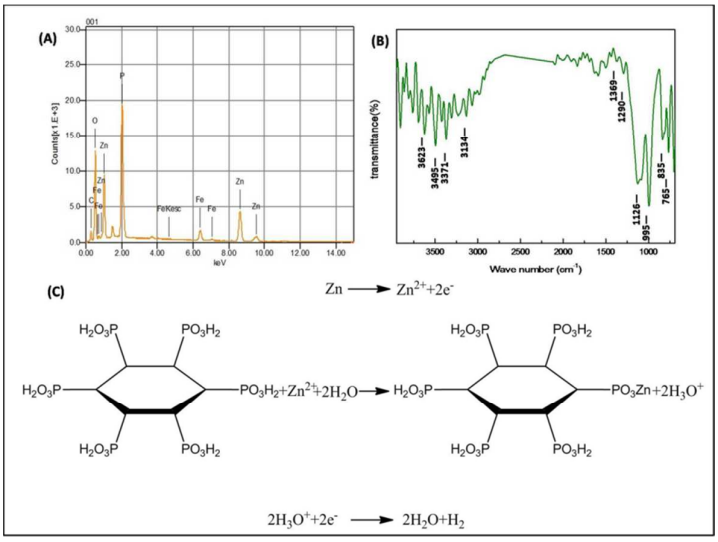
(A)
001
Counts(x1.E+3)
O
P
Zn
Fe
C
FeKesc
Fe
Fe
Zn
Zn
keV
(B)
transmittance(%)
3623
3495
3371
3134
1369
1290
1126
995
835
765
Wave number (cm-1)
(C)
Zn → Zn2++2e-
H2O3P
PO3H2
PO3H2+Zn2++2H2O
PO3Zn+2H3O+
2H3O++2e- → 2H2O+H2

Figure 4

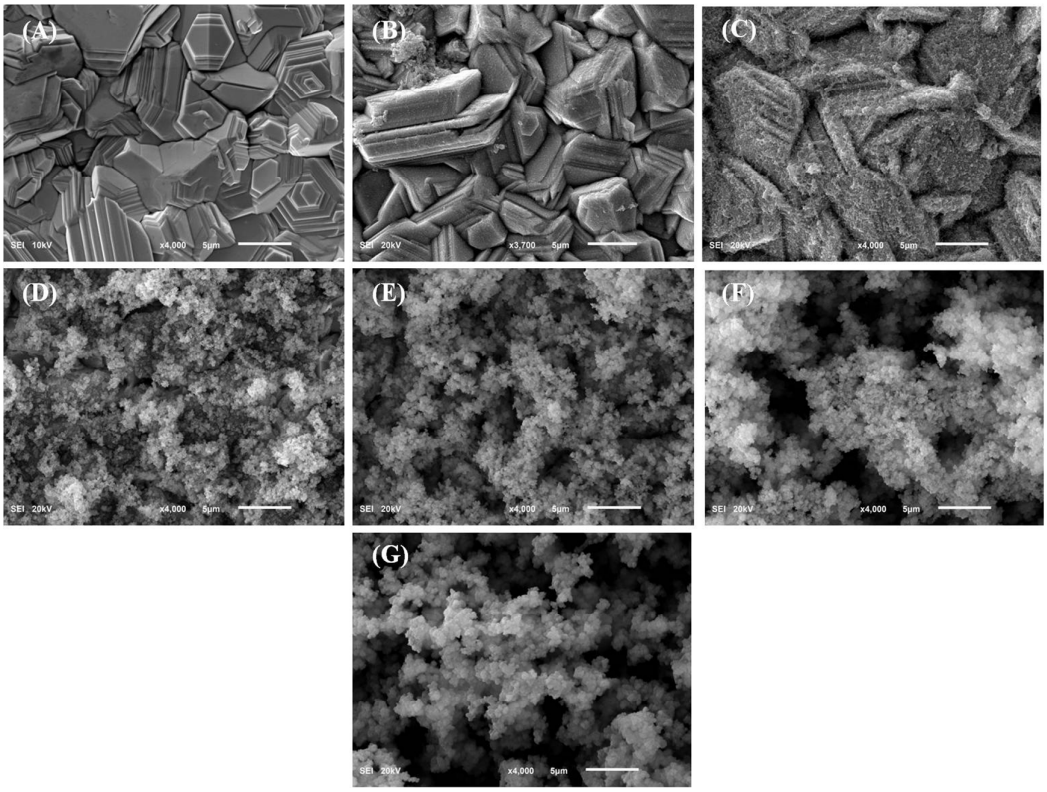
(A)
SEI 10kV x4,000 5μm
(B)
SEI 20kV x3,700 5μm
(C)
SEI 20kV x4,000 5μm
(D)
SEI 20kV x4,000 5μm
(E)
SEI 20kV x4,000 5μm
(F)
SEI 20kV x4,000 5μm
(G)
SEI 20kV x4,000 5μm

Figure 5

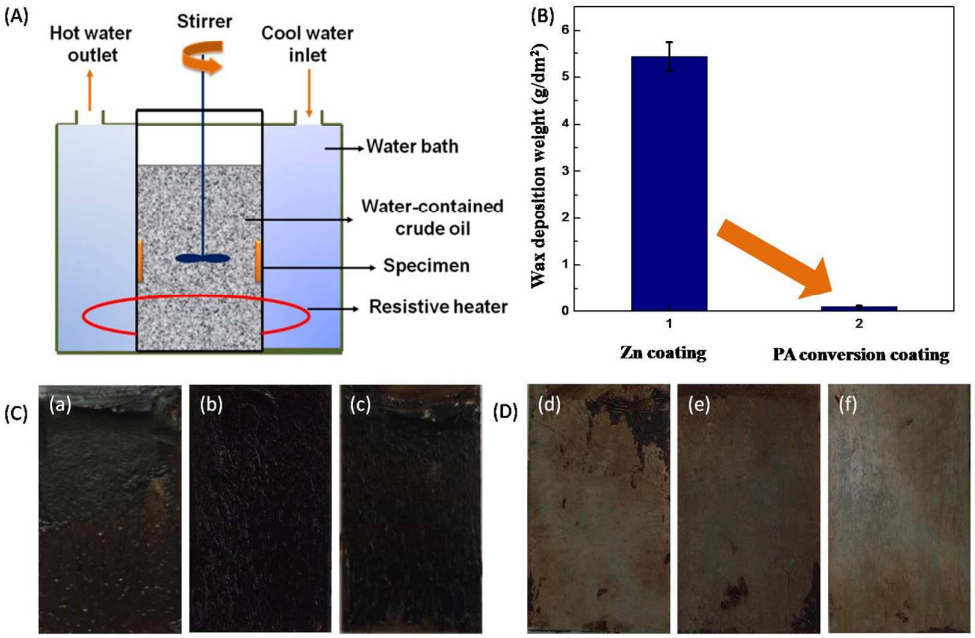
(A)
Hot water outlet
Stirrer
Cool water inlet
Water bath
Water-contained crude oil
Specimen
Resistive heater
(B)
Wax deposition weight (g/dm²)
0
1
2
3
4
5
6
1
2
Zn coating
PA conversion coating
(C)
(a)
(b)
(c)
(D)
(d)
(e)
(f)

Figure 6

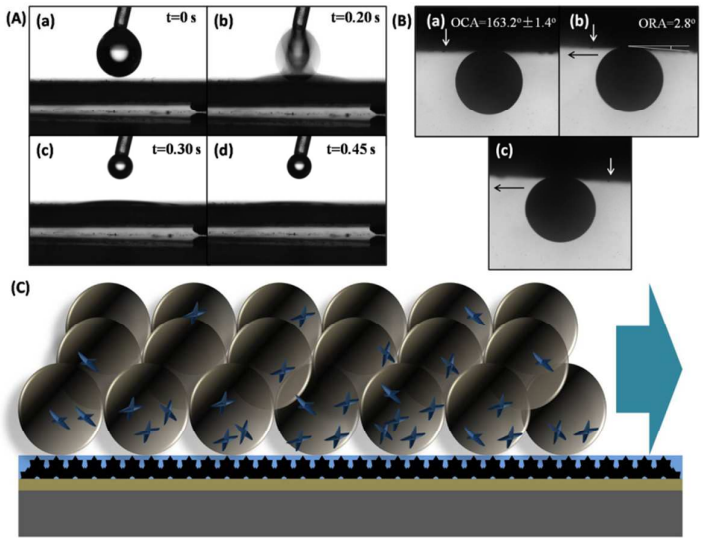

Figure 7

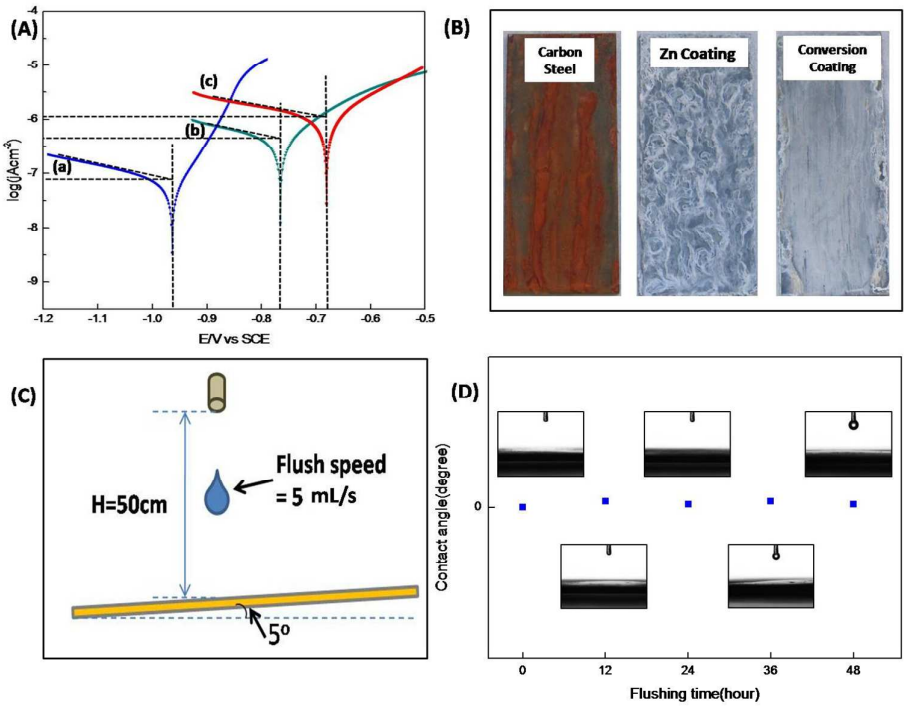
(A)
log(i/Acm-2)
E/V vs SCE
(a)
(b)
(c)
(B)
Carbon Steel
Zn Coating
Conversion Coating
(C)
H=50cm
Flush speed
= 5 mL/s
5°
(D)
Contact angle(degree)
Flushing time(hour)

Figure 8